

# Minutiae Attention Network with Reciprocal Distance Loss for Contactless to Contact-based Fingerprint Identification

Hanzhuo Tan, Ajay Kumar

Department of Computing

The Hong Kong Polytechnic University, Hong Kong

*Abstract: Interoperability between contactless and conventional contact-based fingerprint recognition systems is fundamental for the success of emerging contactless fingerprint technologies which are highly sought, especially due to current pandemic. However, image formation differences and acquisition distortions between these two modalities pose significant challenges for such interoperability. In order to address these challenges, this paper presents a minutiae attention network with Siamese architecture and the reciprocal distance loss function to enable more accurate contactless to contact-based fingerprint identification. The proposed network contains two branches, a global-net branch to recover global features and a minutiae attention branch that focuses on the local minutiae areas. Attention mechanism is introduced to guide the minutiae attention branch to concentrate on distorted areas and recover minutiae/features correspondence for contactless and contact-based fingerprint images from the same fingers. Meanwhile, reciprocal distance loss is specifically designed to impose strong penalty towards contactless and contact-based fingerprint images from different fingers and guide the network to learn robust features for distinguishing identities. Experimental results on two publicly available databases illustrate significant performance improvements, over state-of-art methods in the literature, and validate the effectiveness of the proposed framework for the contactless to contact-based fingerprint identification.*

## 1. Introduction

Fingerprint recognition systems are one of the most widely accepted human identification systems and have a significant share in the biometric market. While conventional contact-based fingerprint systems are widely deployed, limitations like elastic distortion [1] and privacy leakage [2] caused by contact between finger and scanner surface arise the development of contactless fingerprint systems, which acquire the finger images without any physical contact with the scanner. Increasing academic and market interests have been drawn to contactless systems as they offer better hygiene and privacy protection [3] over traditional contact-based systems. However, most legacy databases have been acquired by contact-based sensors, therefore interoperability with contact-based fingerprint is a key challenge for the adoption and development of contactless fingerprint systems.

Early studies on the interoperability [4-9] have reported the challenge of matching fingerprint impressions from different contact-based sensors. While for contactless to contact-

based fingerprint comparison, the recognition rate drops significantly [2, 10-12]. Reference [12] reported 76.44% intra-sensor (contact-based) rank-one identification rate against 16.61% inter-sensor (contact-based versus contactless) rank-one identification rate using open access software [13] in public database [12]. Two key factors, image formation differences and acquisition distortions, contribute to the degradation of recognition rates when comparing contactless with contact-based fingerprint images.

The first factor, image formation differences, denote the fingerprint ridge and valley contrast differences between contactless and contact-based fingerprint images. In contactless systems, reflections of ridges and valleys towards light are recorded by the sensors and form fingerprint images where the boundaries between ridges and valleys are obscured. On the contrary, in contact-based fingerprint systems, contacts between ridges and sensors' surfaces are dominant that high contrast between ridges and valleys is achieved in contact-based images. Such image clarity differences could lead to incoherent feature extraction results for a pair of fingerprint images from the same finger but captured by contactless and contact-based sensors. Consequently, cross-sensor recognition is significantly affected.

The second factor, acquisition distortions regard to pose variations (perspective distortion) [14, 15] in contactless fingerprint systems and elastic distortions for contact-based fingerprint systems. In contactless fingerprint systems, presentations of fingers against sensors are free of control and introduce pose variation as demonstrated in Figure 1. While for contact-based systems, unpredictable finger pressing stress on solid contact-based sensors produces elastic distortions. Transformation/correction from pose variation to elastic distortion is highly non-linear and ill-posed that consequentially contributes to the massive drop of recognition accuracy when matching contactless and contact-based fingerprints. As shown in Figure 2, only small part of region could be aligned between contactless and contact-based fingerprint ridge patterns from the same finger while most pattern correspondence and correlation are distorted.

Other secondary challenges like luminance variance, scale difference and finger placement angle may also affect the interoperability. Data pre-processing techniques can help to address these challenges and this paper will not focus on them.

Although several attempts [16-18] have been made to improve interoperability between contactless and contact-based fingerprint systems, they did not give full consideration to both image formation differences and acquisition distortions. The recognition performance in these methods remained far from security requirement in real work applications. Remarkable success achieved by deep neural network in image classification, segmentation and feature representation [19] has motivated researchers to address biometric recognition problems using trained networks. Superior performance improvements from deep neural networks, over traditional methods that use handcrafted features, have been achieved in face [20, 21], iris [23] and fingerprint [24, 25] recognition. Motivated by the success of deep neural networks, we develop an efficient and accurate contactless to contact-based fingerprint recognition framework to address image formation differences and acquisition distortions.

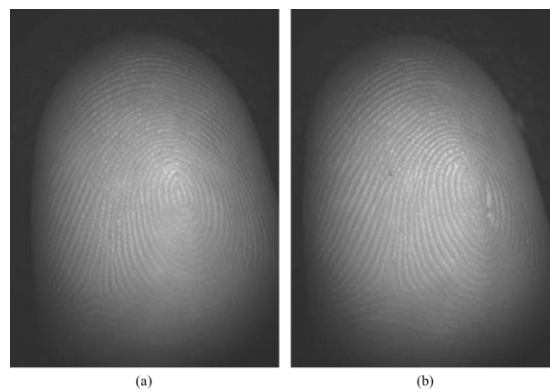


**Figure 1:** Two successively acquired fingerprint images from the completely contactless finger sensor. Significant pose variations can be frequently observed in such contactless fingerprint images and is one of the key challenges to accurately match with contact-based fingerprint images.

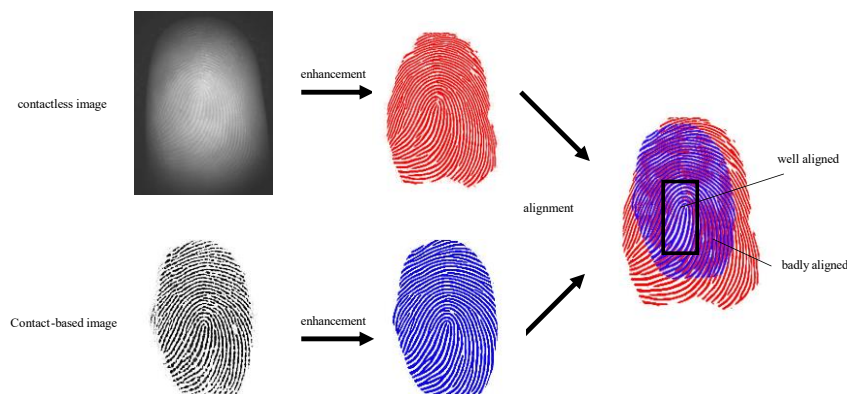


**Figure 2:** Alignment between contactless and contact-based fingerprint images from the same finger. Only very few areas between two modalities can be aligned, largely due to the pose distortions and elastic deformations during the fingerprint sensing.

## 1.1 Related Work

Fingerprint sensor interoperability has attracted increasing attention with the rapid development of sensor technology. There have been many promising investigations on conventional contact-based fingerprint sensor interoperability. Reference [4] presented a pioneer work on sensor interoperability and noticed significant equal error rate (EER) increase from inter-sensor recognition to intra-sensor recognition between an optical and a capacitive sensor. Similarly, reference [5] reported dramatic degradation in the matching performance when comparing fingerprint images from the sweeping thermal and two optical sensors. In order to improve cross-sensor recognition, thin-plate splines (TPS) model was proposed to estimate and compensate deformation between fingerprint images captured by different contact-based sensors [7, 8]. Recently, reference [9] introduced a minutiae descriptor obtained from Gabor filters, a minutiae descriptor from surrounding ridge pattern, and an orientation descriptor obtained from orientation field, to form a robust feature representation for sensor interoperability. Experimental results presented in these methods indicated satisfactory interoperability among contact-based fingerprint sensors, while it's more challenging for contact-based to contactless comparison.

References [6, 26] investigated contactless 3D fingerprint compatibility with legacy ink-on-paper rolled data and reported promising results by using commercial matcher, *Verifinger* [27] on a private database with 38 samples. Technical report [10] presented a thorough evaluation on 498 unique subjects each sampled by four contact-based sensors and three contactless sensors. They demonstrated a significant recognition degradation when matching contactless fingerprints with contact-based fingerprints. Similar interoperability problem was noticed in reference [2, 11, 33], with 30, 150 and 200 subjects respectively. While these works mainly provided evaluation between contactless and contact-based fingerprint recognition, improvements were achieved in [16-18]. Reference [16] employed thin-plate splines to enhance minutiae alignment between contactless and contact-based fingerprint. Although interoperability between contactless and contact-based fingerprint sensor was improved in [16], expensive computation time, i.e. 1.7 seconds for feature extraction and 1.3 seconds for a pair

of matching, was not applicable in deployment. In reference [17], multi-Siamese networks were employed for faster and more accurate cross-sensor fingerprint recognition. Three Siamese networks each trained by fingerprint minutiae image, fingerprint image with blurred core area and core area image respectively were proposed to extract deep-embedded features for recognition based on Euclidian distance. However, core point detection in [17] was executed by commercial software, *Verifinger*, which significantly broke the integrity of a fingerprint recognition system. Recently, reference [18] employed Spatial Transformer Network [28] to compensate the deformation between contactless fingerprint and contact-based fingerprint. Nevertheless, with the use of commercial matcher, only similar cross matching performance compared with [17] was achieved in reference [18].

References [16, 18] attempted to address the acquisition distortions between contactless and contact-based fingerprint images by introduction deformation models. While reference [17] sought to train a network that robust to the acquisition distortions. Nevertheless, references [16-18] failed to account for the image formation differences or could not consider the need for the different minutiae extraction methods for the pair of contactless and contact-based images. The reported recognition accuracy in these references [16-18] is promising but require further improvement for the deployment. Therefore, the objective of this work has been to develop a compact, time-efficient and more accurate contactless to contact-based fingerprint recognition framework, by carefully considering the image formation differences and the acquisition distortions in the corresponding images.

## **1.2 Our Work and Contributions**

This paper develops a minutiae attention network and reciprocal distance loss for more accurate contactless to contact-based fingerprint recognition. The proposed network contains two branches, one *global-net* branch that learns global features from the fingerprint image, another minutiae attention branch, consists of a minutiae detection net (served as attention map) and recognition net, concentrates on local minutiae area. Features extracted from the *global-net* branch and minutiae attention branch are merged and processed by fully-connected layer to

form a final feature vector for an input fingerprint. In order to enhance network robustness, reciprocal distance loss is proposed to impose strong penalty on pair of contactless and contact-based fingerprint images from different fingers. Moreover, contactless fingerprint pose simulation [14] is employed.

The key contributions of this paper can be summarized as the following:

1. A compact contactless to contact-based fingerprint recognition framework consists of a *global-net* branch and minutiae attention branch is proposed to more effectively utilize the global and local fingerprint features. The proposed framework jointly addresses the image formation differences and acquisition distortions in a deep convolutional neural network, which does not require any input (core point detection, minutiae extraction) from commercial software nor relies on commercial matcher as in the previous methods [17,18]. Our reproducible [43] experimental results presented in section 3 indicate a significant performance improvement with the proposed framework, over the previous methods in the literature that relied on commercial software.
2. This is the first work that introduces minutiae attention mechanism into fingerprint recognition. Inspired by the success of attention mechanism in natural language processing [29, 30], researcher employed the mechanism in fingerprint recognition [31, 32]. However, these methods fail to take minutiae, which are the most discriminative fingerprint features widely used in conventional fingerprint recognition, into consideration. In this work, output of minutiae detection net in the minutiae attention branch is specifically designed as an attention map and lead the concentration of recognition net on the local minutiae area. The minutiae detection net is trained by location loss, to predict the likelihood of minutiae existence, as well as regularized by the recognition loss which helps to learn the amount of attention weight that should be assigned. The experiment results presented in section 3 on two public databases consistently demonstrate the effectiveness of minutiae attention mechanism for contactless to contact-based fingerprint identification.
3. The proposed framework addresses the image formation differences and acquisition distortions in four different ways; a) separate minutiae detection net is designed for the

contactless and contact-based fingerprint images. Such separate minutiae extractors, as compared to a general minutiae extractor, can provide more reliable minutiae detection for each fingerprint modality and address ridge-valley contrast differences [44], b) cross-matching recognition loss is imposed to train minutiae detection network, which can enable it to assign attention weights depending on the nature and type of distortion. This loss can enable the recognition network to focus on the minutiae locating in areas highly influenced by acquisition distortions and recover appropriate minutiae set correspondences under the distortion, c) reciprocal distance loss, assigns the loss for a pair of fingerprints with different identities according to the reciprocal of the distance between their feature vectors, encourages the network to learn robust features under the image formation differences and acquisition distortions, d) pose simulation [14] is specifically introduced for the contactless fingerprint images to augment the training samples. Hence a consistent feature extraction against pose variation is achieved for contactless fingerprint.

The rest of this paper is organized as follows. Section 2 introduces the framework of the proposed method and reciprocal distance loss function. The details of experiments are presented in section 3. Key conclusions from this work and further work directions are summarized in section 4.

## **2. Contactless to Contact-based Fingerprint Matching Framework**

This section presents our framework for the proposed contactless to contact-based fingerprint recognition. Image pre-processing steps incorporated for the fingerprint images are briefly introduced, which includes adaptive histogram equalization and spatial transforms. Training data augmentation is then presented, followed by the details of architecture for the proposed network. Finally, the reciprocal distance loss function is discussed.

### **2.1 Data Pre-processing**

Data pre-processing techniques including adaptive histogram equalization and spatial transform are applied to preliminarily address image formation, scale and finger placement

differences between contactless and contact-based fingerprint images.

Spatial transform includes scale normalization, translation and rotation. For contact-based fingerprint image, 500 pixels per inch (dpi) has widely emerged as the standardized image resolution [34, 35] for a range of national ID programs and law-enforcement applications. However, contactless fingerprint sensing, with varying image resolution has been detailed in the literature, e.g. with a low-resolution web camera (~50 dpi) [36] to the high-resolution contactless fingerprint sensing using a commercial camera (~1000 dpi) [39]. Scale normalization between sensed fingerprint images is crucial for interoperability. In this work, a fixed scale normalization factor is adopted for a pair of contactless and contact-based fingerprint sensors to address such scale changes. Translation of core point towards image centre is then performed. Core point detection is achieved by U-net [40], which is trained on labelled training samples in the respective databases. Finally, the rotational alignment among different fingerprints is achieved by normalizing the orientation, or major symmetric axis, of the presented fingers along the vertical direction. Major symmetric axis estimation is performed in two steps, 1) segment fingerprint region from background by detecting pixel intensity larger than a pre-computed threshold, 2) estimate the major axis of the ellipse that has the same second-moments as the fingerprint region, the acquired major axis is the desired fingerprint major symmetric axis. After pre-processing, a preliminary alignment between contactless and contact-based fingerprint images is achieved and the finger placement differences are roughly compensated. More specific details on each of such process are presented in the experimental section.

## **2.2 Training Data Augmentation**

Training data augmentation is designed to improve network robustness towards unexpected variations like luminance, scale, finger placement and pose changes. Augmentation including image rotation, scaling, luminance adjustment is firstly performed. Moreover, pose simulation [14] is specifically employed for contactless fingerprint images to compensate finger pose variations between the different fingerprint captures, which are mainly caused by



uncontrollable finger presentation towards contactless fingerprint sensor. As shown in Figure 3, an input 2D contactless fingerprint image can be modelled by a 3D ellipsoid. Rotation of ellipsoid in 3D space can simulate such frequently observed pose variations and generate (respective) synthetic contactless 2D fingerprint images. Experimental results presented in section 3.2 demonstrate that such pose simulation based data augmentation can significantly help to improve cross matching performance and validate its effectiveness for compensating the acquisition distortions.

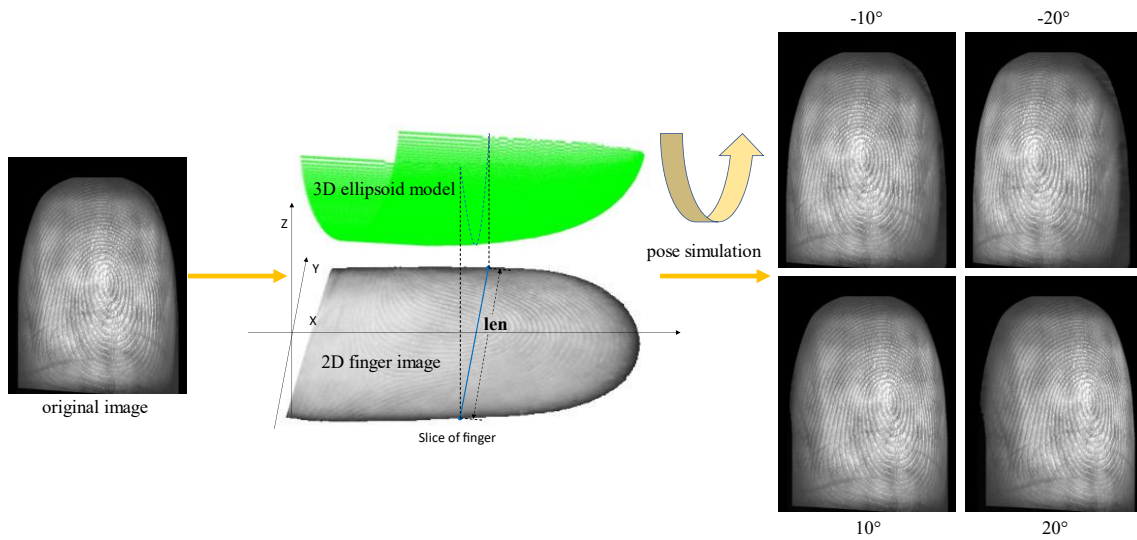


**Figure 3:** Flow diagram for the contactless fingerprint training images data augmentation. A 3D ellipsoid model is estimated from a given 2D contactless image. Then pose simulation is performed in the 3D space to generate different synthetic contactless 2D images corresponding to the different poses from the same finger.

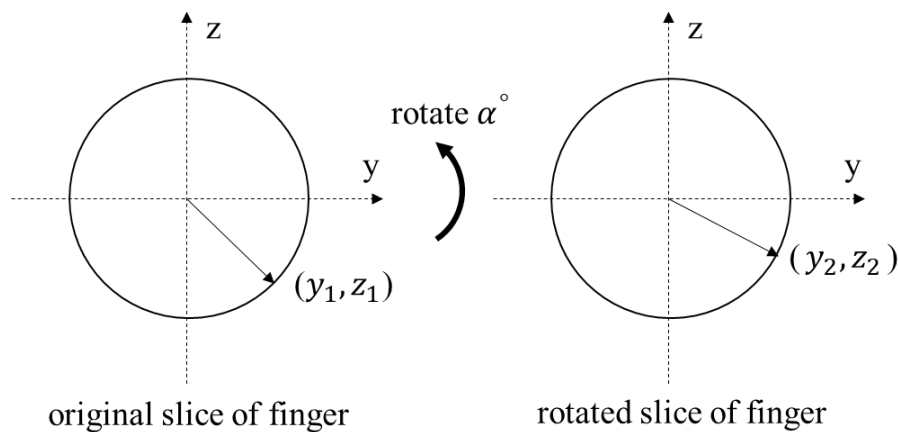


**Figure 4:** Rotation for each slice of finger. Each point  $(y_1, z_1)$  in the original slice of finger is rotated into  $(y_2, z_2)$ . The pixel intensity value of each point  $(y_2, z_2)$  can be obtained by tracking back to point  $(y_1, z_1)$  in the original slice.

The radius of each slice in ellipsoid model is directly estimated from contactless fingerprint image as shown in Figure 3 (*len*). Figure 4 demonstrates the simulation of such pose changes. Each point in a slice of finger is rotated in 3D space with the following equation.

$$\begin{bmatrix} y_1 \\ z_1 \end{bmatrix} = \begin{bmatrix} \cos(\alpha) & \sin(\alpha) \\ -\sin(\alpha) & \cos(\alpha) \end{bmatrix} \times \begin{bmatrix} y_2 \\ z_2 \end{bmatrix} \quad (1)$$

where  $\alpha$  represents the rotation angle for pose simulation. The pose simulation inherently introduces artefacts and pose simulation for large angle should be avoided.

### 2.3 Cross Fingerprint Matching Network

Reference [17] presented multi-Siamese framework for the contactless to contact-based fingerprint recognition. However, the multi-Siamese framework contains three Siamese networks and each network is trained separately. This framework [17] is quite complex. Therefore, in this work we consider a concise and compact cross fingerprint matching network which is detailed in the following section.

#### 2.3.1 Conventional Siamese Network

A basic contactless to contact-based fingerprint matching Siamese network (*global-net*) is summarized in Figure 5. This *global-net* serves as a baseline for evaluation of the attention mechanism which will be discussed in the section 2.3.2.

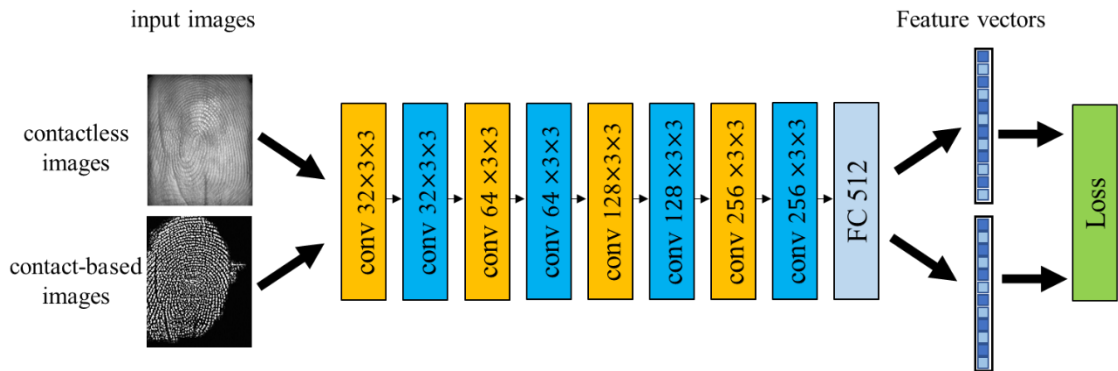


**Figure 5:** Contactless to contact-based fingerprint matching network architecture (*global-net*). Convolutional layers with blue colour have the stride of 2.

The *conv* operator in above figure refers to the convolutional layer, *FC* denotes fully connected layer, each convolutional layer is followed by batch normalization layer, *ReLU* activation and

dropout layer. This network is trained in Siamese manner, i.e. a pair of deep representation feature vectors is generated from a pair of contactless and contact-based fingerprint images (two-channel input data) to generate loss for the network training. In such Siamese architecture, pair of images from the same finger will lead the network to extract more discriminative features against image formation differences and acquisition distortions. While pair of images from different finger will guide the network to learn distinguishable identities.

### **2.3.2 Siamese Network with Minutiae Attention**

The proposed *global-net* could achieve promising matching accuracy between contactless and contact-based fingerprint images. Neurons in convolutional layers of *global-net* are exposed to the whole fingerprint image and extract global features that represent the fingerprint. However, as shown in Figure 5, high dissimilarities, or image formation differences significantly affect the success of extracting coherent features for fingerprint images from the same finger but captured by contactless and contact-based sensors.

In conventional fingerprint identification systems, minutiae, i.e. fingerprint ridge bifurcation or termination points, are one of the most prominent and robust features and widely adopted for the recognition. Therefore, it's judicious to include such spatial location information for cross matching and minutiae attention branch is proposed, i.e. a minutiae detection net is employed to generate minutiae likelihood map that served as attention map and encourages the neurons to obtain local robust features. Architecture for minutiae detection net is shown in Figure 6 and summarized in Table 1. In order to better address image formation differences, separate minutiae networks are trained for contactless and contact-based fingerprint images respectively.

Features from *global-net* (without *FC* layer) and minutiae attention branch are added and processed by fully-connected layer to form a 512-dimension vector as the final representation for the input image. The overall framework that contains *global-net* and minutiae attention branch is shown in the Figure 7.

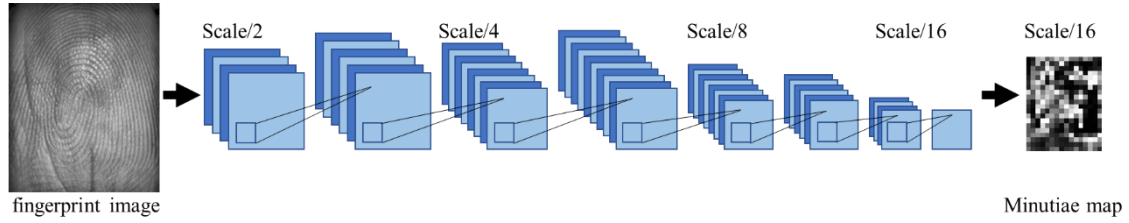


**Figure 6:** Illustration for the minutiae detection network. The value of predicted minutiae map in each position represents the attention that recognition neurons should assign to that area.

**Table 1:** Minutiae network architecture.

Layer	Filter Size	Output Number	Stride
Conv1	3	32	2
Conv2	3	64	1
Conv3	3	128	2
Conv4	3	256	1
Conv5	3	128	2
Conv6	3	64	1
Conv7	3	32	2
Conv8	3	1	1

Each convolutional layer is followed by batch normalization layer, *ReLU* activation and dropout layer. The last convolutional layer, *Conv8*, is followed by sigmoid layer.

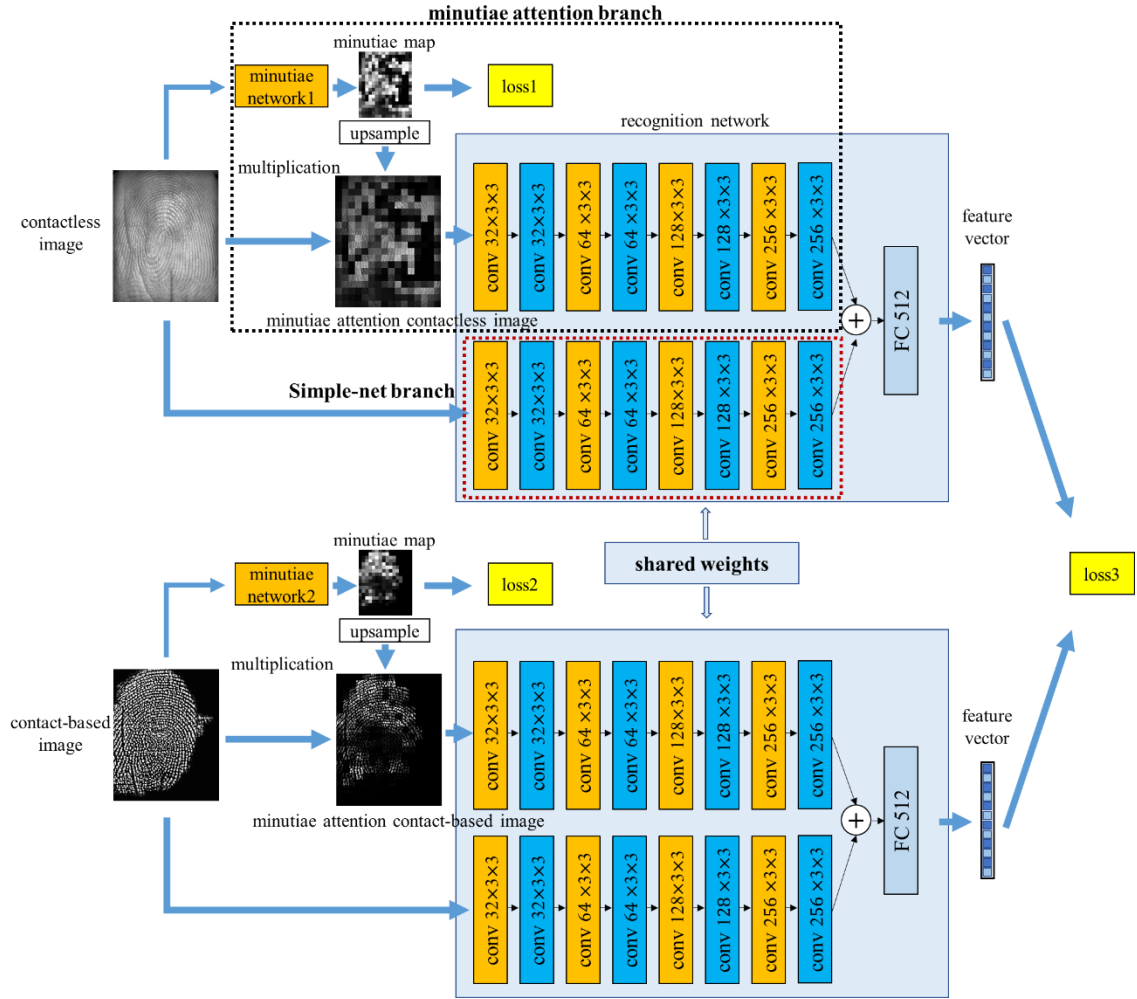


**Figure 7:** Overall framework for the contactless to contact-based fingerprint recognition network. The global-net branch uses the original image as input while minutiae attention branch uses the image with the minutiae attention of the input. The recognition network, located in light-blue rectangle, is trained using the Siamese architecture.

As shown in Figure 6, each point on the minutiae map indicates the probability of minutiae existence in a  $16 \times 16$  pixels area on the original fingerprint image. The minutiae map is up-sampled to the original input size and serves as attention map to force the recognition neurons in minutiae attention branch focusing on potential minutiae areas.

The image formation differences could be addressed by introducing minutiae attention branch, while acquisition distortions, or pose variances and elastic distortions are addressed by introducing recognition loss and location loss for the training of minutiae networks. In Figure-2, it demonstrates that most pattern correspondence and correlation between contactless and contact-based fingerprint samples from the same finger are distorted due to acquisition distortions. Hence the attention weight for each area should be distributed not only according

to its probability of minutiae existence, but also related to the its distortion and potential contribution for the recognition. Areas with high distortions should be investigated and assigned higher weights. Failure of recovering correspondence for these distorted areas is the main contributor to the degradation of matching performance. On the contrary, reliable undistorted and clean areas should be depressed and given low attentions since information/correspondence in these areas could be easily detected by the *global-net* branch. A fixed minutiae prediction network could not learn any information about distortions. As a result, recognition loss is also imposed to the training of minutiae networks to encourage them to assign the attention weights intelligently according to the distortions and potential contributions for recognition.

Intuitively, training of minutiae networks and recognition network could be performed jointly in the same time and the training process is summarized in Algorithm 1.

**Algorithm 1:** Joint training algorithm for our network

1. Pretrain minutiae network1 and minutiae network2 for contactless and contact-based fingerprint.
2. Update minutiae network1, minutiae network2 and recognition network together with  $Loss=loss1+loss2+loss3$ .

Minutiae networks and recognition network are dependent to each other, i.e. minutiae prediction results will affect the feature extract direction of recognition network, while recognition loss will influence the training of minutiae network, jointly training for all the networks could not converge well. Hence in this work, starting from roughly trained minutiae networks and fingerprint recognition network, an iterative and progressive algorithm that optimizes minutiae detection and fingerprint recognition networks is proposed and summarized in the following Algorithm 2.

**Algorithm 2:** Iterative training algorithm for our network

1. Pretrain minutiae network1 and minutiae network2 for contactless and contact-based fingerprint.
2. Fix minutiae network1 and minutiae network2, update recognition network with  $loss3$ .
3. Fix recognition network, update minutiae network1 and minutiae network2 with  $Loss=loss1+loss2+loss3$ .
4. Perform step 3 and step 4 iteratively.

Meanwhile, a conventional attention model which has no constrain on the minutiae is evaluated for comparison with the minutiae attention model. In this conventional attention model, the attention network will only be updated by the recognition loss. For the name consistency, attention network will still be written as ‘minutiae network’. The training of conventional attention model is summarized in the following Algorithm 3.

**Algorithm 3:** Conventional attention model

1. Fix minutiae network1 and minutiae network2, update recognition network with  $loss3$ .
2. Fix recognition network, update minutiae network1 and minutiae network2 with  $Loss= loss3$ .
3. Perform step 3 and step 4 iteratively.

where recognition network represents the proposed network except minutiae network1 and minutiae network2,  $loss1$  and  $loss2$  are the cross-entropy loss between prediction and ground truth minutiae score map,  $loss3$  is the proposed reciprocal distance loss which will be discussed in the following section.

Manually marked minutiae are required to train the minutiae networks, however, no public labelled contactless to contact-based fingerprint database is available. In order to obtain labelled data with reasonable human labour, a week minutiae label scheme is introduced. Patch-

based minutiae detection [14] is employed to generate weak minutiae ground truth label. Details will be presented in experimental section and this network is named as minutiae ground truth network to distinguish with minutiae network in the proposed contactless to contact-based fingerprint recognition framework.

## 2.4 Reciprocal Distance Loss Function

Loss function could implicitly force the network to learn robust feature against image formation differences and acquisition distortions. Contrastive loss function [37] is widely employed to train Siamese network. Let  $(I_1, I_2)$  as a pair of contactless fingerprint and contact-based fingerprint image for input of Siamese network.  $Y = 0$  represents  $I_1$  and  $I_2$  belong to the same finger (genuine pair), while  $Y = 1$  regards  $I_1$  and  $I_2$  are samples taken from different fingers (imposter pair). Contrastive loss can be written in the following.

$$\text{Contrastive loss} = (1 - Y)d(N(I_1, I_2))^2 + Y \max(M - d(N(I_1, I_2)), 0)^2 \quad (2)$$

where  $N$  represents the Siamese network,  $d(N(I_1, I_2))$  is distance measurement for a pair of feature vectors,  $M$  denotes the margin. For each input pair  $(I_1, I_2)$ , network  $N$  would encode the images into a pair of deep feature representations respectively. The loss for genuine pair will be  $d(N(I_1, I_2))^2$ , while for imposter pair, the loss  $\max(M - d(N(I_1, I_2)), 0)^2$  focuses on pairs that have smaller distance than margin  $M$ .

The contrastive loss only set margin for imposters, double margin contrastive loss [38] also set constrain on the genuine pairs and can be written as following.

$$\begin{aligned} \text{Double margin loss} = & (1 - Y) \max(d(N(I_1, I_2)) - M_1, 0)^2 \\ & + Y \max(M_2 - d(N(I_1, I_2)), 0)^2 \end{aligned} \quad (3)$$

In reference [17], the double margin loss is named as distance-aware loss. Compared with contrastive loss, this loss also focuses on genuine pair with similarity larger than given margin  $M_1$ . Hence it aims to concentrate on the challenging genuine pairs with large distance (low similarity) and imposter pairs with small distance (high similarity).

In order to improve the feature distinguishability learned by the network, the similarity of



imposter pair should be small, i.e. stronger penalty should be assigned to imposter pair with high similarity (small distance). The original contrastive loss or double margin loss does not distinguish much on the very high similarity (small distance) for imposter pairs, therefore, reciprocal distance loss is proposed.

$$\begin{aligned} \text{Reciprocal distance loss} = & (1 - Y) \max(d(N(I_1, I_2)) - M_1, 0)^2 \\ & + Y \min\left(\max\left(\frac{1}{d(N(I_1, I_2))} - M_2, 0\right), M_3\right)^2 \end{aligned} \quad (4)$$

In the proposed reciprocal distance loss function, loss for the imposter pair is related to the multiplicative inverse of distance measurement and significant penalty is assigned to imposter pair with high similarity (small distance). It aims to focus on the training of very challenging imposter samples to ensure feature distinguishability. In such way, the match score overlapping region between genuine and imposter pairs could be further increased and recognition improvement is expected. In order to prevent gradient overflow for imposter pair with extreme similarity (extreme small distance), a threshold  $M_3$  is set to the loss. The results in the Experiments section illustrate the effectiveness of proposed loss compared over other loss functions.

## 2.5 Generate Match Score

Denote feature vectors extracted from proposed network as  $f_1$  and  $f_2$  respectively for a pair of contactless and contact-based fingerprints. The match score  $s$  between the respective fingerprint feature vectors  $f_1, f_2$  can be calculated as follows,

$$s = \frac{1}{d(f_1, f_2)} \quad (5)$$

where the  $d(f_1, f_2)$  represents the distance calculation between the feature vectors  $f_1$  and  $f_2$ . As compared to conventional fingerprint matching algorithms, the match score generated from distance measurement between feature vectors is much faster and favourable for the large-scale search, identification or de-duplication applications.

### 3. Experiments and Results

In this section, detailed experimental results are presented to evaluate the effectiveness of proposed framework and reciprocal distance loss function on two public databases [12, 39]. Our implementation is based on Pytorch, with Adam optimizer with learning rate at  $10^{-4}$ . Euclidian distance is selected for distance measurement. We empirically fix the margins,  $M_1 = 0.5$ ,  $M_2 = 1$ ,  $M_3 = 5$ , for all the experiments in this section.

#### 3.1 Contactless and Contact-based Fingerprint Databases

The first database [12] contains 5760 contactless and corresponding contact-based fingerprint images acquired from 320 fingers. Similar to reference [17], 160 fingers each with 12 contactless and contact-based fingerprint samples are selected as training samples. While the rest 160 fingers each with 6 contactless and contact-based fingerprint samples are used for testing. In the training samples, images from first 16 training fingers are selected for validation. In the second database [39], 500 fingers each with 2 contactless and 4 contact-based fingerprint samples are used for testing, and the rest fingers each with 2 contactless and 4 contact-based fingerprint samples are used for fine-tuning the network trained by database [12], images from first 100 training fingers are selected for validation. Original resolution of database [12] is  $2048 \times 1536$  and  $356 \times 328$  for contactless and contact-based fingerprint image respectively. Original resolution of database [39] is  $1280 \times 1024$  and  $640 \times 480$  for contactless and contact-based fingerprint image respectively.



**Figure 8:** Typical fingerprint samples. top row: contactless fingerprint images, bottom row: corresponding contact-based fingerprint images.

Data pre-processing includes adaptive histogram equalization and spatial transform. Follow reference [12], scale of contactless data in database [12] is normalized by down sample factor of 0.25 and 0.5 for database [39]. Translation of core point towards image centre is then performed. Finally, image rotation is achieved by rotating the major symmetric axis of fingerprint perpendicular against the image row. Threshold for segmenting finger region is set as 45 in database [12] and 30 in database [39]. Contactless fingerprint training sample augmentation is achieved using  $\pm 10, \pm 20$  pose simulation samples. In order to achieve image size consistency, all images are cropped into  $320 \times 256$  as final input size to the network. For generating weak minutiae label as discussed in section 2.3, 50 images in each four databases (contactless and contact-based fingerprint database in [12] and [39]) are manually labelled. Then a patch-based minutiae ground truth network [14] is trained and employed for the prediction of the rest fingerprint samples in each database. Such minutiae prediction results are used as ground truth for training minutiae networks in the proposed contactless to contact-based fingerprint recognition framework. Note that only a weak minutiae ground truth is extracted in this process and the minutiae networks are expected to produce spurious results as the training labels are not ideal.

### 3.2 Experimental Evaluations

In order to evaluate the proposed contactless to contact-based fingerprint matching framework, experiments are performed for the verification and identification. Experimental protocols, training and testing set selection for both tasks are exactly the same as in reference [17]. Verification task in database [12] generates 5760 ( $160 \times 6 \times 6$ ) genuine scores and 915840 ( $160 \times 6 \times 159 \times 6$ ) imposter scores, while for database [39], a total of 4000 ( $500 \times 2 \times 4$ ) genuine scores and 1996000 ( $500 \times 2 \times 499 \times 4$ ) imposter scores are generated from the test data. The first sample in contactless database is used as gallery for identification task. Receiver Operating Characteristic (ROC) Cumulative Match Characteristic (CMC) compared with results reported in reference [17] is presented in Figure 9 and Figure 10. In order to perform fair comparison against commercial software, *Verifinger* [27], the same down sample factors for contactless databases are adopted, also the same experimental protocols are applied.

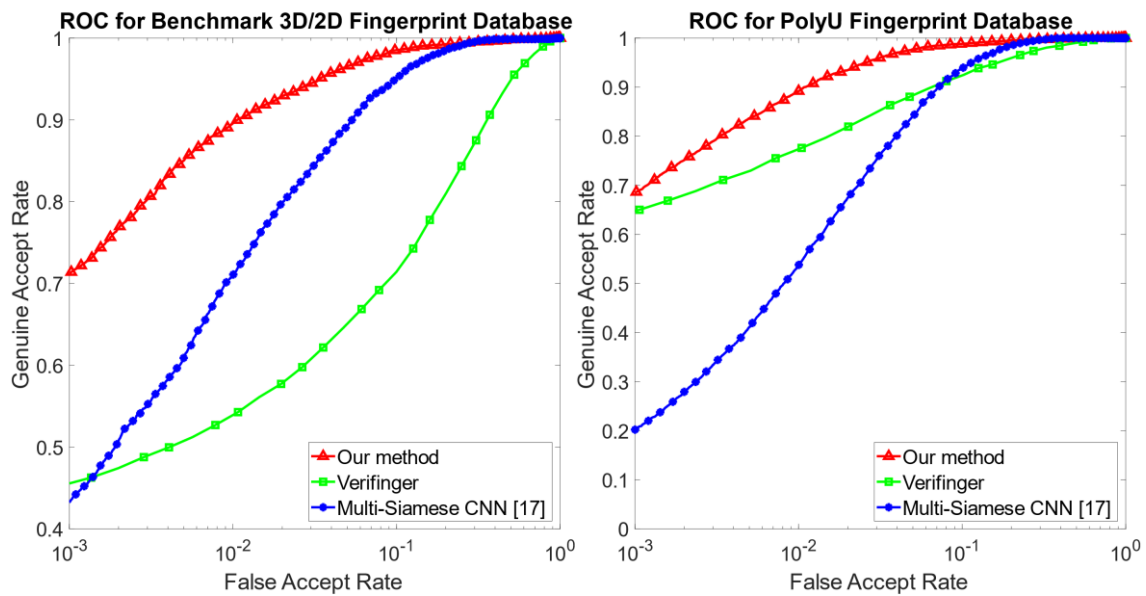


**Figure 9:** ROC comparison between proposed method, *Verifinger*, and method in reference [17] in Benchmark 3D/2D fingerprint Database [39] and PolyU Contactless to Contact-based Fingerprint Database [12].

**Table 2:** Summary of recognition rate and Equal Error Rate for experiments in Figure 9.

Method/Database	Benchmark 3D/2D fingerprint Database [39]		PolyU Contactless to Contact-based Fingerprint Database [12]	
	GAR@ FAR=10 <sup>-3</sup>	GAR@ FAR=10 <sup>-3</sup>	GAR@ FAR=10 <sup>-3</sup>	EER
Proposed method	<b>72.0%</b>	<b>68.5%</b>	<b>68.5%</b>	<b>4.13%</b>
Verifinger [27]	46.0%	64.8%	64.8%	19.31%
Multi-Siamese CNN [17]	45.2%	20.3%	20.3%	7.11%

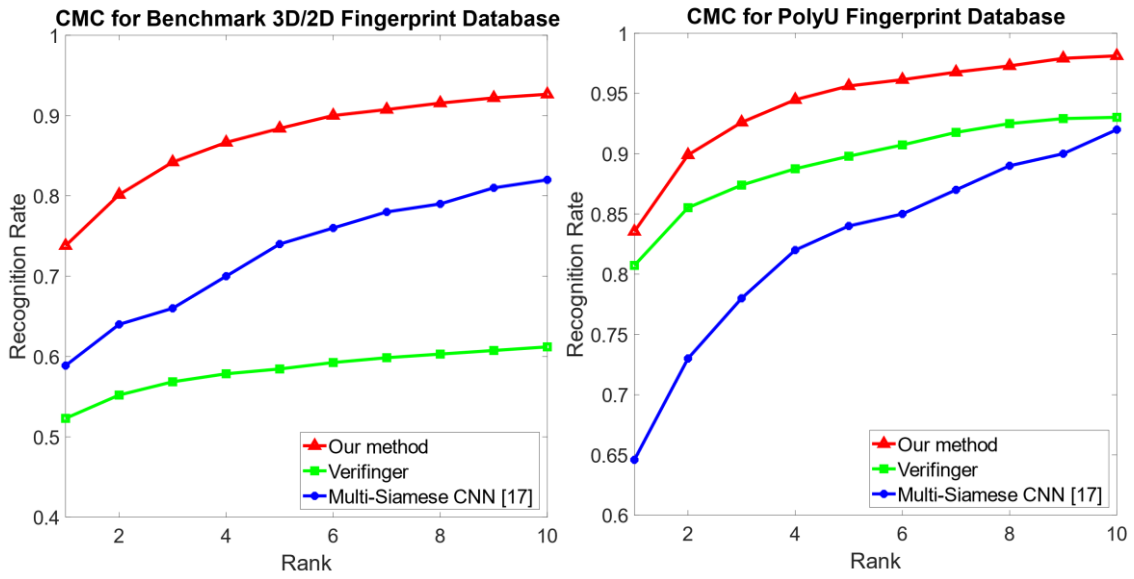


**Figure 10:** CMC comparison between proposed method, *Verifinger*, and method in reference [17] in Benchmark 3D/2D fingerprint Database [39] and PolyU Contactless to Contact-based Fingerprint Database [12].

**Table 3:** Rank-one accuracy for experiments in Figure 10.

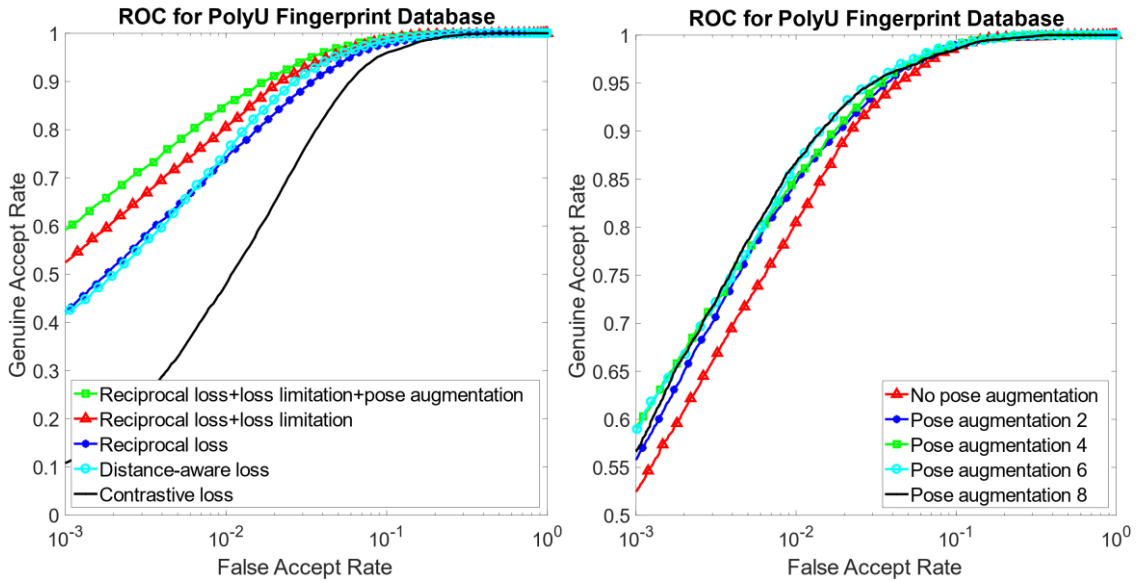
Method/Database	Benchmark 3D/2D fingerprint Database [39]	PolyU Contactless to Contact-based Fingerprint Database [12]
Proposed method	<b>73.80%</b>	<b>83.54%</b>
Verifinger [27]	52.30%	80.73%
Multi-Siamese CNN [17]	58.87%	64.59%

From Figure 9 and Figure 10, it could be clearly observed that proposed method significantly

outperforms all previous methods. The rank-one accuracy increases 3.48% over *Verifinger* and 29.34% over previous state-of-the-art [17] in database [12]. While in database [39], 41.11% and 25.36% increment over *Verifinger* and [17] are achieved.

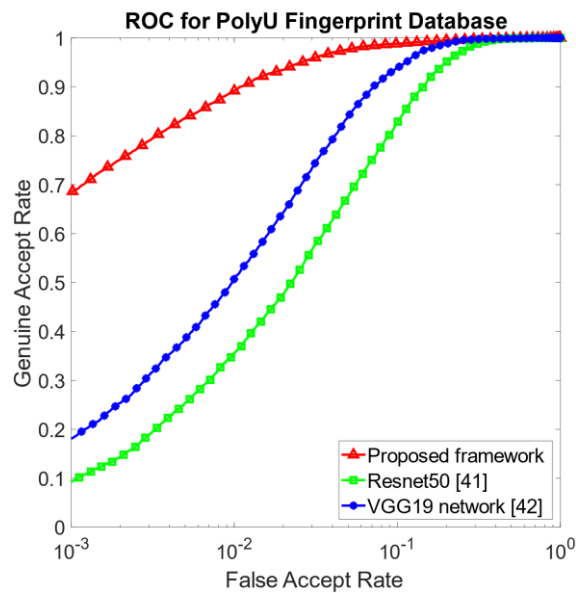
The contribution of each process in proposed method is systematically investigated and the corresponding ROCs are shown in Figure 11(a). All the experimental results in this figure use the same *global-net* as shown in Figure 5. Firstly, contrastive loss is employed for training the network and the respective results are shown in the ROC labelled as ‘Contrastive loss’. Then the distance-aware loss proposed in [17] is used and results are presented from the ROC labeled as ‘Distance-aware loss’. Then a simple reciprocal distance loss without limitation ( $M_3 = +\infty$ ) is employed, and the corresponding results are labeled as ‘Reciprocal loss’. Followed by the reciprocal distance loss with limitation ( $M_3 = 5$ ) and the respective results are labeled as ‘Reciprocal loss+loss limitation’. Finally, contactless fingerprint pose augmentation is adopted, with the training loss as reciprocal loss with limitation ( $M_3 = 5$ ), and respective results are labeled as ‘Reciprocal loss+loss limitation+pose augmentation’.

In addition, contactless pose augmentation is also investigated and respective results are presented in Figure 11(b). The ROC with label ‘Pose augmentation 2’ in this figure refers to the case when the training contactless fingerprint image is augmented to its nearest  $\pm 10^\circ$  poses, label ‘Pose augmentation 4’ represents such augmentation with  $\pm 10^\circ$ ,  $\pm 20^\circ$  poses, label ‘Pose augmentation 6’ means augmented to  $\pm 10^\circ$ ,  $\pm 20^\circ$ ,  $\pm 30^\circ$  poses, and ‘Pose augmentation 8’ label indicates pose augmentation with  $\pm 10^\circ$ ,  $\pm 20^\circ$ ,  $\pm 30^\circ$ ,  $\pm 40^\circ$  poses. Furthermore, comparative performance evaluation of the proposed minutiae attention network against the two popular deep learning architectures, Resnet50 [41] and VGG19 [42], is provided in Figure 11(c). Similar analysis has been studied in [17] but those networks were trained with the cross-entropy loss. Hence in this work, the Resnet50 [41] and VGG19 [42] are trained in Siamese manner with the proposed reciprocal distance loss.



(a)

(b)



(c)

**Figure 11:** (a) ROC curves for analysis of each process in proposed method. (b) ROC curves for investigation of pose augmentation. (c) ROC curves for comparison with other popular deep learning architectures.

Clearly from Figure 11(a), (b), the proposed reciprocal loss and data augmentation for contactless fingerprint significantly enhance the contactless to contact-based fingerprint recognition performance. The experiments of pose augmentation rate illustrated in Figure 11(b) indicate that high rates of augmentation (‘Pose augmentation 6’ and ‘Pose augmentation 8’) do

not further improve the matching performance as pose augmentation artifacts are serious for large degree of simulation. From Figure 11 (c), similar conclusion with reference [17] could be drawn, both Resnet50 [41] and VGG19 [42] could not converge well for the specific cross-sensor task. The loss function comparison is provided in Figure 12. In loss for genuine pair, the proposed loss is relatively small among all losses. It specially focuses on genuine pair that has a large distance (low similarity). As for imposter pair, reciprocal distance loss has a relatively large loss especially for challenging pair with small distance (high similarity). While in traditional contrastive loss or distance-aware loss (double margin contrastive loss), as shown in Figure 12, penalty for small distance is relatively slight, which leads to poor performance on low FAR, i.e. large intersection for genuine and imposter scores. In Figure 12, it indicates that for imposter pair with extremely small distance (around 0.1), the loss would be overwhelming and potentially harmful for the convergency of network. Impose a limitation for such extreme distance significantly contributes to the cross-matching performance as shown in Figure 11(a), the ‘Reciprocal loss’ against ‘Reciprocal loss + loss limitation’.

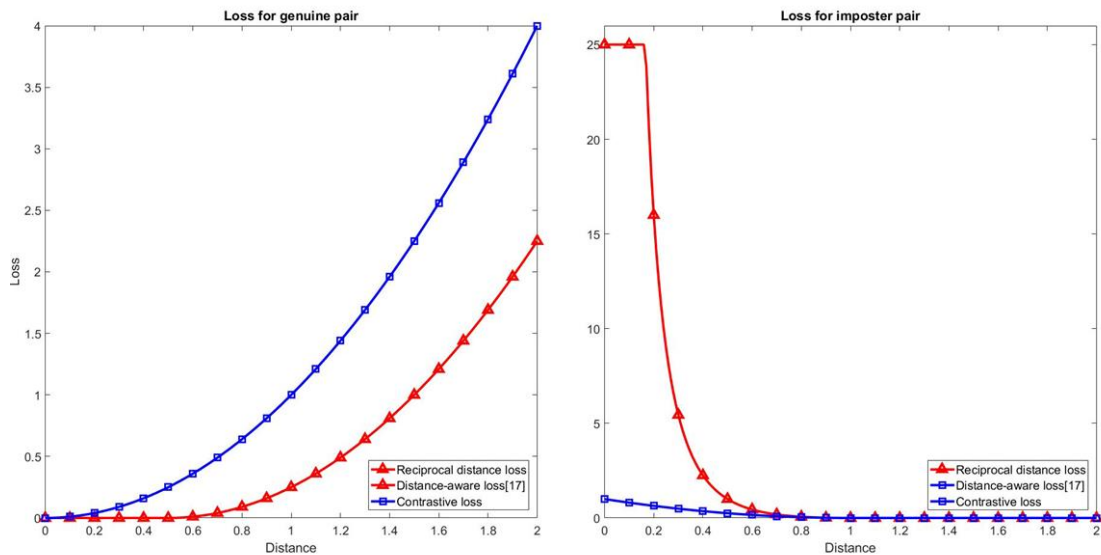


**Figure 12:** Illustration of different loss function.

Furthermore, the comparative evaluation of *global-net* and minutiae attention branch is an be observed from the results in Figure 13, Figure 14 and Table 4. The *global-net* introduced in section 2.3 is firstly evaluated and labelled as ‘*Global-net*’. Then the proposed framework



trained by Algorithm-1 and Algorithm-2 is evaluated and labelled as ‘Proposed framework trained with Algorithm 1’ and ‘Proposed framework trained with Algorithm 2’ respectively. A fixed minutiae network which would not be updated is investigated and labelled as ‘Proposed framework with fixed minutiae network’. Conventional attention model trained with Algorithm-3 is also evaluated and labelled as ‘Proposed framework with conventional attention’. From Table 4, it demonstrates that minutiae branch could significantly enhance the contactless to contact-based fingerprint interoperability and 6.92% rank-one rate improvement is achieved over *global-net* in database [12] while 9.99% rank-one rate increment in database [39]. While for the proposed framework with fixed minutiae network, it could not converge. As discussed in section 3.1, the minutiae ground truth labels are far from ideal. Accordingly, the messy minutiae attention maps will significantly distort the focus of network and contribute to the failure of training. As for the conventional attention model, it does not contribute to the cross matching. For the training Algorithm-1, jointly training could not converge either as expected.

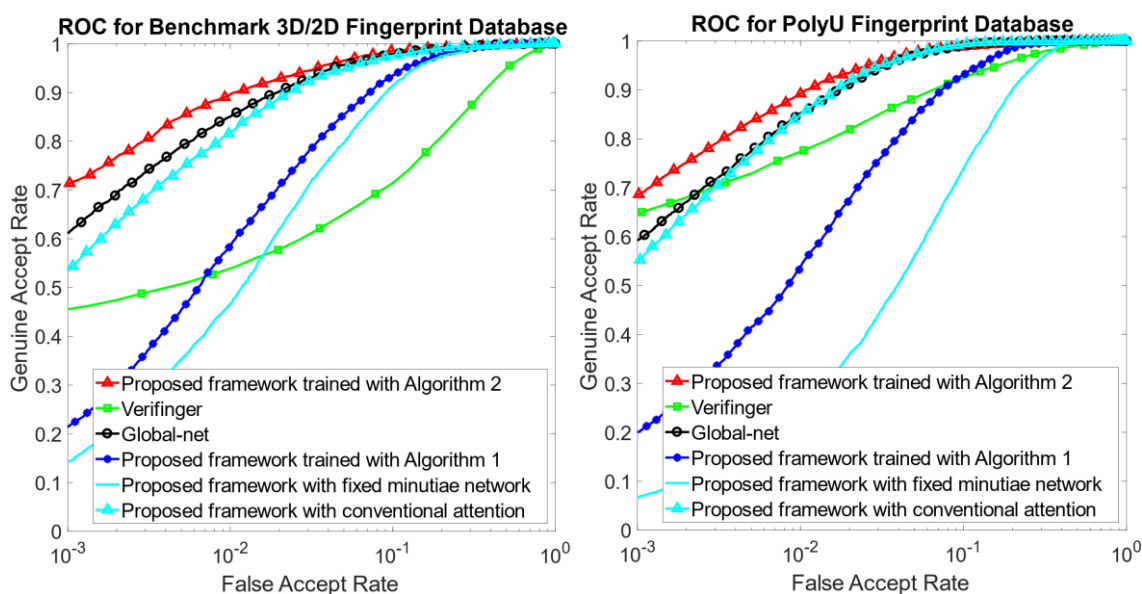


**Figure 13:** ROC comparison between different training strategies and network architectures of proposed network in Benchmark 3D/2D fingerprint Database [39] and PolyU Contactless to Contact-based Fingerprint Database [12].

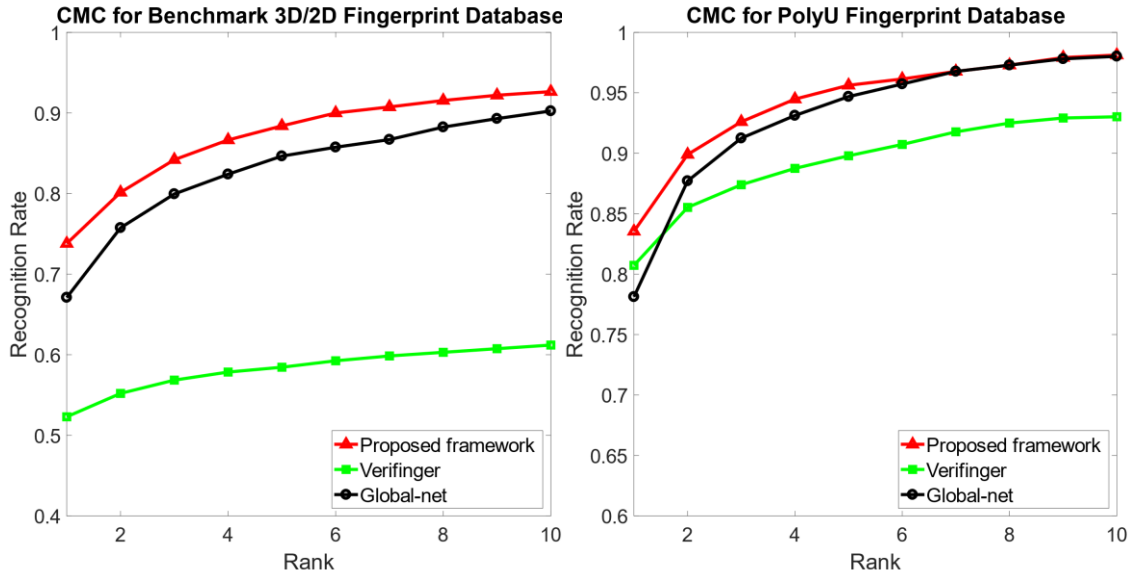


**Figure 14:** CMC comparison between different training strategies and network architectures of proposed network in Benchmark 3D/2D fingerprint Database [39] and PolyU Contactless to Contact-based Fingerprint Database [12].

**Table 4:** Summary on the average rank-one recognition accuracy from experiments.

Method/Database	Benchmark 3D/2D fingerprint Database [39]	PolyU Contactless to Contact-based Fingerprint Database [12]
<i>global-net</i> (baseline)	67.10%	78.13%
proposed framework	<b>73.80%</b>	<b>83.54%</b>

A comparison of pretrained/fixed minutiae network prediction results and proposed trainable minutiae network prediction results is presented in Figure 15. Compare to the fixed minutiae network, the trainable minutiae network assigns higher weights to distorted areas. In such a way, *global-net* branch would extract features on global and clean areas while minutiae attention branch could focus on distorted local areas and recover correspondence. Hence features learned from two branches are relatively independent and significantly help to improve the recognition between contactless and contact-based fingerprint images.

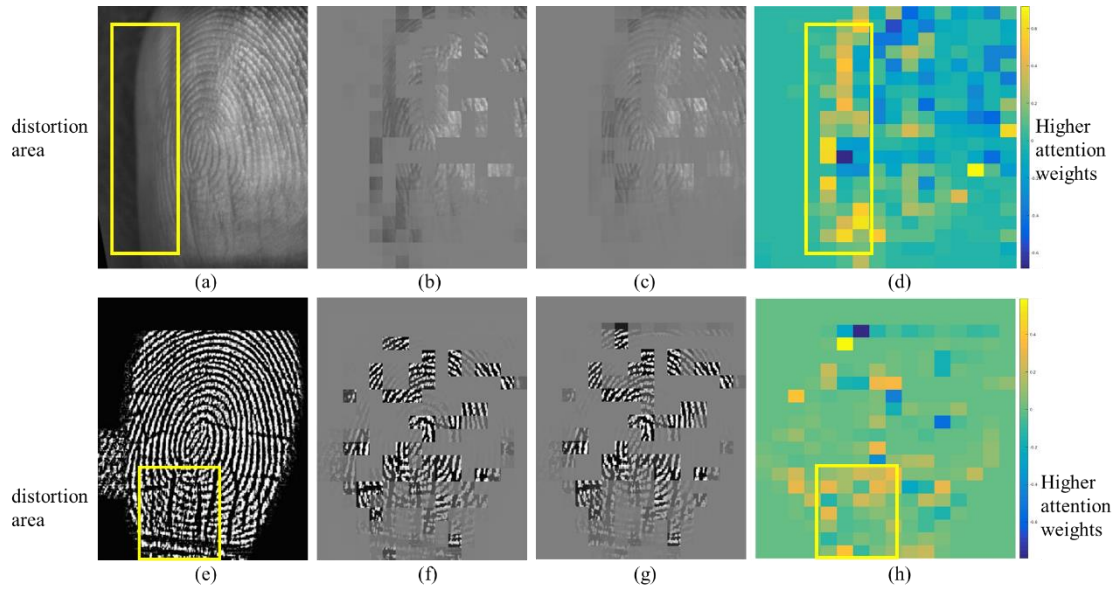


**Figure 15:** Comparison between pretrained/fixed minutiae network and trainable minutiae network. (a), (e) are the contactless and contact-based fingerprint respectively. (b), (f) are the corresponding minutiae attention results from trainable minutiae network. (c), (g) are the corresponding minutiae attention results from fixed minutiae network. (d), (h) are the difference between minutiae predictions from trainable network and fixed network, where blue refers to lower attention value in trainable network result, yellow refers to higher attention value in trainable network.

### 3.3 Discussion

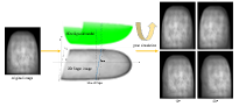
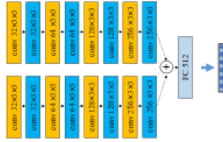
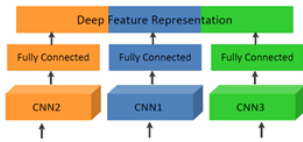
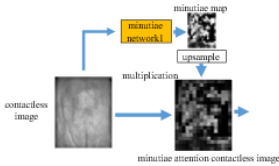

This sub-section presents more insights on the comparisons with the earlier methods that have appeared in the literature. This discussion also presents additional experimental results and is organized in four sub-sections, *i.e.* Multi-Siamese Network, image enhancement, deformation correction and time complexity. These insights can help to further validate the value of the proposed approach to address contactless to contact-based fingerprint interoperability problem.

#### 3.3.1 Multi-Siamese Network

The proposed method is inspired by reference [17], which adopt a Multi-Siamese Network to improve interoperability. However, the only similarity between our method and method in reference [17] is the use of Siamese architecture, which is a universal mechanism that widely used for training the deep neural networks. We claim our novelty over reference [17] mainly from three perspectives. First, we propose a single feature extraction network, while reference [17] is an ensemble method, which sums up weighted identification scores obtained from three

networks to generate a final match score. Thus, our network offers significant improvement from the perspective of network integrity. Second, we introduce minutiae attention mechanism into fingerprint recognition. In reference [17], the minutiae information is converted into a minutiae image where each minutia is represented as a circle and short orientation line. Such representation cannot consider the contribution differences among minutiae towards the identification and is vulnerable to spurious minutiae. Finally, we propose a reciprocal distance loss which assigns strong penalty to the imposter pairs with higher similarity (smaller distance). While in reference [17], conventional double margin loss is adopted which may not help to adequately distinguish very similar imposter pairs. Experiments presented in Figure 11 indicate the superiority of reciprocal distance loss over double margin loss or the distance-aware loss. A more detailed differences between our method and reference [17] are also summarized in the Table 5.

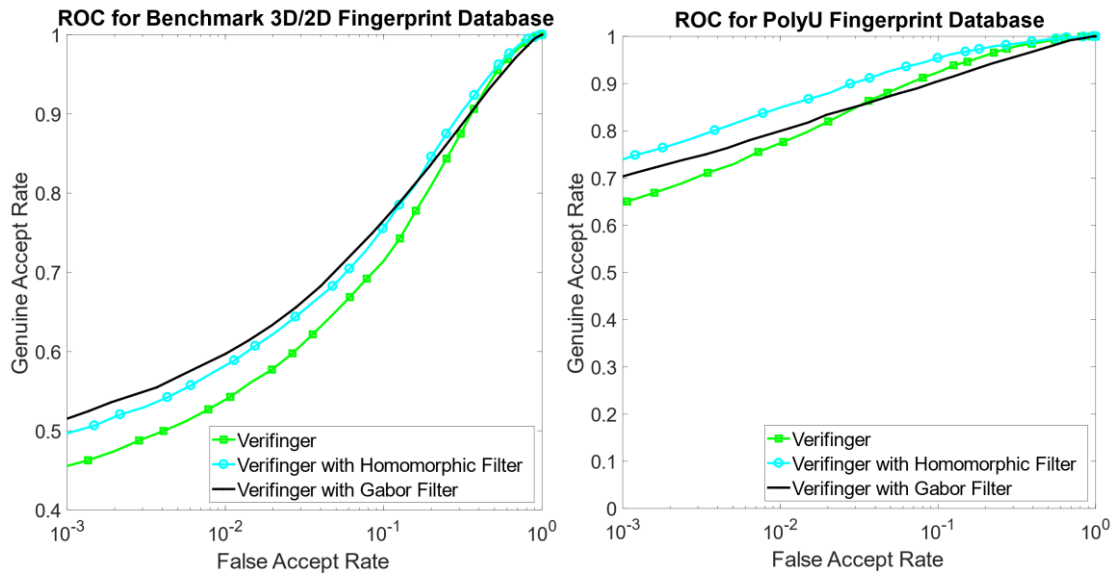
**Table 5:** Comparison between proposed method and method in reference [17]

	Proposed method	Reference [17]
Contactless pose variances (Section 2.2)		no
Feature extraction (Section 2.3)	<p>Single network</p> 	<p>Three networks</p> 
Minutiae interpretation (Section 2.3)	<p>Minutiae attention</p> 	<p>Fixed minutiae image</p> 
Loss function (Section 2.4)	<p>Reciprocal distance loss</p> $(1 - Y) \max(d(N(I_1, I_2)) - M_1, 0)^2 + Y \min(\max\left(\frac{1}{d(N(I_1, I_2))} - M_2, 0\right), M_3)^2$	<p>Conventional double margin loss</p> $(1 - Y) \max(d(N(I_1, I_2)) - M_1, 0)^2 + Y \max(M_2 - d(N(I_1, I_2)), 0)^2$
Match score generation	$S = Dis(f_1, f_2)$	<p>Ensemble method</p> $S = w_1 * Dis(f_{11}, f_{12}) + w_2 * Dis(f_{21}, f_{22}) + w_3 * Dis(f_{31}, f_{32})$
Dependency	No	Rely on <i>Verifinger</i>
Performance	Outperform commercial software	Much worse than commercial software

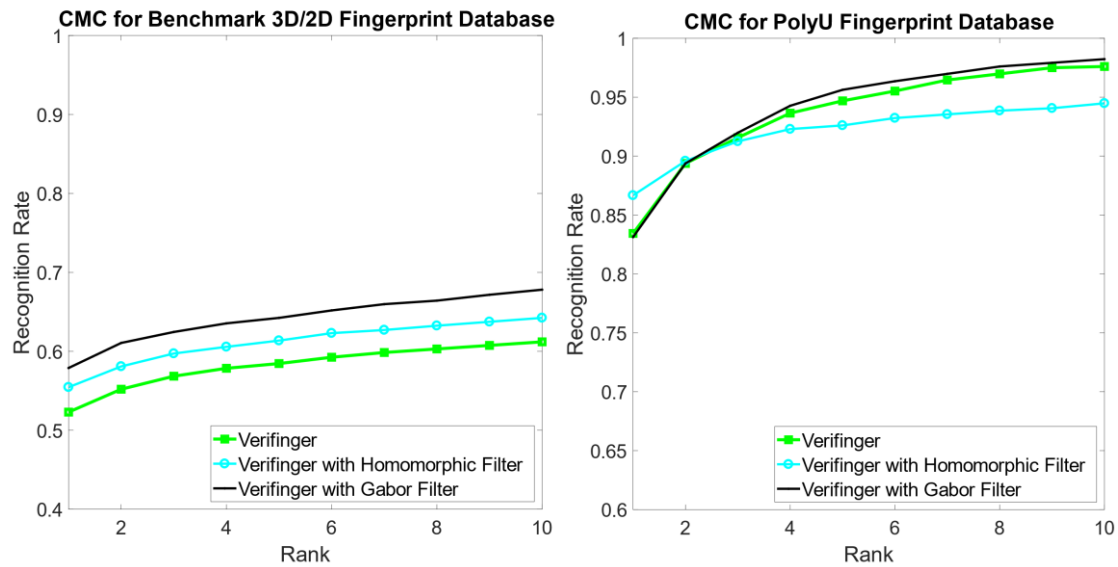
### 3.3.2 Image Enhancement

Image enhancement, specifically the homomorphic [26] and Gabor filtering, techniques are widely adopted for the contactless fingerprint identification [22] to reduce noise and improve the matching accuracy. In order to verify the contribution of image enhancement towards interoperability, homomorphic filter and Gabor filter-based approach were incorporated for the contactless fingerprint images before using *Verifinger* matcher and respective results are presented in Figure 16 and Figure 17. The ROC with label ‘Verifinger with Homomorphic Filter’ refers to the case when Homomorphic Filter is applied to the contactless fingerprint images before using *Verifinger*, similarly, ‘Verifinger with Gabor Filter’ refers to the case when

Gabor filter based image enhancement is incorporated.



**Figure 16:** ROC comparison for image enhancement in Benchmark 3D/2D fingerprint Database [39] and PolyU Contactless to Contact-based Fingerprint Database [12].



**Figure 17:** CMC comparison for image enhancement in Benchmark 3D/2D fingerprint Database [39] and PolyU Contactless to Contact-based Fingerprint Database [12].

**Table 6:** Comparative Equal Error Rate for experiments in Figure 16.

Method/Database	Benchmark 3D/2D fingerprint Database [39]	PolyU Contactless to Contact-based Fingerprint Database [12]
<i>Verifinger</i> [27]	19.31%	8.62%
<i>Verifinger</i> with Gabor Filter	17.46%	10.07%
<i>Verifinger</i> with Homomorphic Filter	17.56	6.59%

From the Figure 16-17, it can be observed that with the use of enhancement step, *Verifinger* can perform slightly better than without enhancement step. In general, our proposed method (Figure 9-10) has comparable performance against the commercial software with image enhancement techniques.

### 3.3.3 Deformation Correction

We also evaluated approaches in the literature [12], [18] which can enhance the interoperability by increasing similarity between contactless and contact-based fingerprint images. Reference [12], [18] both incorporate thin-plate splines (TPS) to perform deformation correction between these two modalities. In reference [12], a robust TPS is proposed and its parameters are estimated from minutiae correspondence between contactless and contact-based fingerprint. Reference [18] is inspired by spatial transformer network [28] and the parameters for TPS are learned during the network training. The performance of these two works on the database [39] is summarized in the Figure 18.

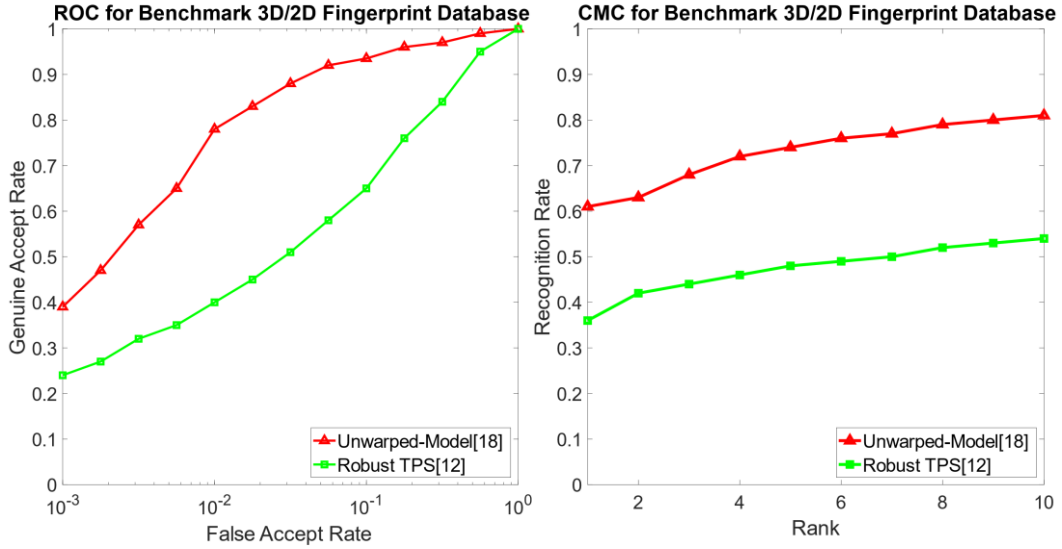


**Figure 18:** ROC and CMC results for method in reference [12], [18].

As compare to the results in Figure 9 and Figure 10, it can be observed that our proposed method can achieve state-of-the-art performance and significantly outperforms over the methods in reference [12], [18].

### 3.3.4 Time Complexity

Comparative evaluation on the complexity using running time comparisons was also performed and these results are summarized in Table 7. All our experiments were run on an Intel i5 CPU with NVIDIA 2080Ti GPU. These results can help to further validate the merit of the proposed approach over earlier methods in the literature.

**Table 7:** Summary on run time comparisons.

Method	Preprocessing per image	Feature extraction per image	Matching per pair
Proposed method	0.198s	<b>0.0032s</b>	<b><math>0.92 \times 10^{-5}s</math></b>
<i>Verifinger</i> [27]	0.130s	0.6000s	$2.50 \times 10^{-5}s$
Multi-Siamese CNN [17]	1.710s	0.0092s	$1.27 \times 10^{-5}s$
Robust TPS [12]	Included in feature extraction	1.6820s	1.26s
Unwarped-Model [18]	0.144s	0.6000s	$2.50 \times 10^{-5}s$



#### 4. Conclusions and Future Work

This work proposes a faster and accurate deep-neural-network-based framework for improving the interoperability between contactless fingerprint sensor and conventional contact-based fingerprint sensors. The minutiae attention network, along with the reciprocal distance loss, proposed in this work can explicitly addresses image formation differences and acquisition distortions. Our experimental results presented in previous section, on two publicly available databases, indicate significantly better performance than the previous methods and a popular commercial software, with 29.34% rank-one accuracy improvement over previous state-of-the-art [17], 3.48% over *Verifinger* [27], on database [12] and 25.36% increment over [17], 41.11% over *Verifinger* [27], on database [39]. These promising results significantly improve the contactless to contact-based fingerprint interoperability which can contribute to the rapid adoption and development of contactless fingerprint techniques. Limited by the quantity of contactless fingerprint image samples in publicly available databases, generalization of the trained network towards new database needs further work and improvement.

Despite promising results and advancements in the cross-fingerprint matching capabilities in this paper, achieved matching accuracy needs further improvement. Therefore, further work is required to 1) improve robustness of framework, i.e. cross-database evaluation without fine-tuning, 2) accounting for the elastic distortions in contact-based fingerprint images and developing advanced algorithms to overcome the challenges from the involuntary pose variations and elastic distortions.

#### References

- [1] A. M. Bazen, and S. H. Gerez, "Fingerprint matching by thin-plate spline modelling of elastic deformations," *Pattern Recognition*, vol. 36, no. 8, pp. 1859-1867, 2003.
- [2] R. D. Labati, A. Genovese, V. Piuri, and F. Scotti, "Toward unconstrained fingerprint recognition: A fully touchless 3-D system based on two views on the move," *IEEE transactions on systems, Man, cybernetics: systems*, vol. 46, no. 2, pp. 202-219, 2015.
- [3] R. D. Labati, V. Piuri, and F. Scotti, "Touchless fingerprint biometrics (Series in Security, Privacy and Trust)," Boca Raton, FL, USA: CRC Press, 2015, pp. 185-187.
- [4] A. Ross, and A. Jain, "Biometric sensor interoperability: A case study in fingerprints," *Proc. Int. ECCV Workshop Biometric Authentication*, 2004, pp. 134-145.

- [5] F. Alonso-Fernandez, R. N. Veldhuis, A. M. Bazen, J. Fierrez-Aguilar, and J. Ortega-Garcia, "Sensor interoperability and fusion in fingerprint verification: A case study using minutiae-and ridge-based matchers," *Proc. 9th Int. Conf. Control, Automat., Robot. Vis.*, 2006, pp. 1-6.
- [6] Y. Chen, G. Parziale, E. Diaz-Santana, and A. K. Jain, "3D touchless fingerprints: Compatibility with legacy rolled images," *Proc. 2006 Biometrics Symp. Biometric Consortium Conf.*, 2006, pp. 1-6.
- [7] A. Ross, and R. Nadgir, "A thin-plate spline calibration model for fingerprint sensor interoperability," *IEEE Transactions on Knowledge Data Engineering*, vol. 20, no. 8, pp. 1097-1110, 2008.
- [8] A. Ross and R. Nadgir, "A calibration model for fingerprint sensor interoperability," in *Proc. SPIE Conf. Biometric Technology for Human Identification III*, Orlando, FL, Apr. 2006, pp. 62 020B-1–62 020B-12.
- [9] H. Alshehri, M. Hussain, H. A. Aboalsamh, and M. A. Al Zuair, "Cross-sensor fingerprint matching method based on orientation, gradient, and Gabor-HoG descriptors with score level fusion," *IEEE Access*, vol. 6, pp. 28951-28968, 2018.
- [10] L. Ericson, and S. Shine, *Evaluation of contactless versus contact fingerprint data phase 2 (version 1.1)*, vol. 249552, I. ManTech Advanced Systems International, DOJ Office Justice Programs, 2015.
- [11] W. Zhou, J. Hu, S. Wang, I. Petersen, and M. Bennamoun, "Performance evaluation of large 3D fingerprint databases," *Electronics Letters*, vol. 50, no. 15, pp. 1060-1061, 2014.
- [12] C. Lin, and A. Kumar, "Matching contactless and contact-based conventional fingerprint images for biometrics identification," *IEEE Transactions on Image Processing*, vol. 27, no. 4, pp. 2008-2021, 2018.
- [13] C. I. Watson, M. D. Garris, E. Tabassi, C. L. Wilson, R. M. McCabe, S. Janet, and K. Ko, *User's guide to NIST biometric image software (NBIS)*: NIST, 2007.
- [14] H. Tan, and A. Kumar, "Towards More Accurate Contactless Fingerprint Minutiae Extraction and Pose-Invariant Matching," *IEEE Transactions on Information Forensics and Security*. vol. 15, pp. 3924 - 3937, June 2020.
- [15] R. D. Labati, A. Genovese, V. Piuri, and F. Scotti, "Contactless fingerprint recognition: a neural approach for perspective and rotation effects reduction," in *Proc. IEEE Workshop Computational Intell. in Biometrics and Identity Management (CIBIM)*, 2013, pp. 22-30.
- [16] C. Lin, and A. Kumar, "Improving cross sensor interoperability for fingerprint identification," *Proc. Int. Conf. Pattern Recognit. (ICPR)*, 2016, pp. 943-948.
- [17] C. Lin, and A. Kumar, "A CNN-based framework for comparison of contactless to contact-based fingerprints," *IEEE Transactions on Information Forensics and Security*, vol. 14, no. 3, pp. 662-676, 2018.
- [18] A. Dabouei, S. Soleymani, J. Dawson, and N. M. Nasrabadi, "Deep Contactless Fingerprint Unwarping," *Proc. Intl. Conf. on Biometrics*, ICB 2019, pp. 1-8, 2019.
- [19] Y. LeCun, Y. Bengio, and G. Hinton, "Deep learning," *nature*, vol. 521, no. 7553, pp. 436-444, 2015.
- [20] Z. Liu, P. Luo, X. Wang, and X. Tang, "Deep learning face attributes in the wild," in *Proc.*

- Int. Conf. Comput. Vis. (ICCV)*, 2015, pp. 3730-3738.
- [21] Y. Sun, Y. Chen, X. Wang, and X. Tang, "Deep learning face representation by joint identification-verification," *Proc. Adv. Neural Inf. Process. Syst. (NIPS)*, 2014, pp. 1988-1996.
- [22] A. Kumar, *Contactless 3D Fingerprint Identification*, Springer, 2018.
- [23] Z. Zhao, and A. Kumar, "Towards more accurate iris recognition using deeply learned spatially corresponding features," in *Proc. Int. Conf. Comput. Vis. (ICCV)*, 2017, pp. 3809-3818.
- [24] R. F. Nogueira, R. de Alencar Lotufo, and R. C. Machado, "Fingerprint liveness detection using convolutional neural networks," *IEEE transactions on Information Forensics and Security*, vol. 11, no. 6, pp. 1206-1213, 2016.
- [25] Y. Tang, F. Gao, J. Feng, and Y. Liu, "Fingernet: An unified deep network for fingerprint minutiae extraction," in *Proc. IEEE Int. Joint Conf. Biometrics (IJCB)*, 2017, pp. 108-116.
- [26] G. Parziale, and Y. Chen, "Advanced technologies for touchless fingerprint recognition," *Handbook of Remote Biometrics*, London, U.K: Springer, 2009, pp. 83-109.
- [27] S. D. K. Verifinger. (2010). Neuro Technology. [Online]. Available: <http://www.neurotechnology.com/verifinger.html>.
- [28] M. Jaderberg, K. Simonyan, and A. Zisserman, "Spatial transformer networks," in *Proc. Adv. Neural Inf. Process. Syst. (NIPS)*, 2015, pp. 2017-2025.
- [29] D. Bahdanau, K. Cho, and Y. J. a. p. a. Bengio, "Neural machine translation by jointly learning to align and translate," *Proc. Int. Conf. Learn. Representations (ICLR)*, 2015.
- [30] A. Vaswani, N. Shazeer, N. Parmar, J. Uszkoreit, L. Jones, A. N. Gomez, Ł. Kaiser, and I. Polosukhin, "Attention is all you need," in *Proc. Adv. Neural Inf. Process. Syst. (NIPS)*, 2017, pp. 5998-6008.
- [31] L. Pang, J. Chen, F. Guo, Z. Cao, and H. Zhao, "ROSE: Real One-Stage Effort to Detect the Fingerprint Singular Point Based on Multi-scale Spatial Attention," *arXiv preprint arXiv:03918*, 2020.
- [32] S. Banerjee, and S. Chaudhuri, "DeFraudNet: End2End Fingerprint Spoof Detection using Patch Level Attention," *Proc. of IEEE Winter Conference on Applications of Computer Vision (WACV)*, 2020, pp. 2695-2704.
- [33] J. Libert, J. Grantham, B. Bandini, K. Ko, S. Orandi, and C. Watson, "Interoperability Assessment 2019: Contactless-to-Contact Fingerprint Capture," NIST, Tech. Report NISTIR 8307, Gaithersburg, MD, USA, April , 2020.
- [34] D. Maio, D. Maltoni, R. Cappelli, J. L. Wayman, and A. K. Jain, "FVC2004: Third fingerprint verification competition," *Proc. Int. Conf. Biometric Authentication*, ICBA 2004, pp. 1-7, Hong Kong, 2004.
- [35] R. Cappelli, M. Ferrara, A. Franco, and D. Maltoni, "Fingerprint verification competition 2006," *Biometric Technology Today*, vol. 15, no. 7-8, pp. 7-9, 2007.
- [36] A. Kumar, and Y. Zhou, "Contactless fingerprint identification using level zero features," *Proc. IEEE Conf. Comput. Vis. Pattern Recognit.*, 2011, pp. 114-119, 2011.
- [37] S. Chopra, R. Hadsell, and Y. LeCun, "Learning a similarity metric discriminatively, with application to face verification," *Proc. IEEE Conf. Comput. Vis. Pattern Recognit.*, CVPR 2005, pp. 539-546, 2005.

- [38] F. Sadeghi, C. L. Zitnick, and A. Farhadi, "Visalogy: Answering visual analogy questions," *Proc. Adv. Neural Inf. Process. Syst.*, NIPS 2015, pp. 1882-1890, 2015.
- [39] W. Zhou, J. Hu, I. Petersen, S. Wang, and M. Bennamoun, "A benchmark 3D fingerprint database," *Proc. 11th Int. Conf. Fuzzy Syst. Knowl. Discovery (FSKD)*, 2014, pp. 935-940.
- [40] O. Ronneberger, P. Fischer, and T. Brox, "U-net: Convolutional networks for biomedical image segmentation," *Proc. Med. Image Comput. Comput. -Assisted Intervention (MICCAI)*, 2015, pp. 234-241.
- [41] K. He, X. Zhang, S. Ren, and J. Sun, "Deep residual learning for image recognition," *Proc. IEEE Conf. Comput. Vis. Pattern Recognit. (CVPR)*, 2016, pp. 770-778.
- [42] K. Simonyan, and A. Zisserman, "Very deep convolutional networks for large-scale image recognition," *arXiv preprint arXiv:1409.1556*, 2014.
- [43] Weblink for downloading codes for the algorithms in this paper, <http://www.comp.polyu.edu.hk/~csajaykr/attentionFP.zip>
- [44] R. Vyas, A. Kumar, "A collaborative approach using ridge-valley minutiae for more accurate contactless fingerprint identification," *arXiv preprint arXiv:1906.06045*, 2019.